

# Investigating atmospheric photochemistry in the Johannesburg-Pretoria megacity using a box model

## AUTHORS:

Alexandra S.M. Lourens<sup>1</sup>

Tim M. Butler<sup>2</sup>

J. Paul Beukes<sup>1</sup>

Pieter G. van Zyl<sup>3</sup>

Gerhard D. Fourie<sup>4</sup>

Mark G. Lawrence<sup>2</sup>

## AFFILIATIONS:

<sup>1</sup>Unit for Environmental Sciences and Management, North-West University, Potchefstroom, South Africa

<sup>2</sup>Institute for Advanced Sustainability Studies, Potsdam, Germany

<sup>3</sup>School of Physical and Chemical Sciences, North-West University, Potchefstroom, South Africa

<sup>4</sup>EnviroNgaka, Brits, South Africa

## CORRESPONDENCE TO:

Pieter van Zyl

## EMAIL:

pieter.vanzyl@nwu.ac.za

## POSTAL ADDRESS:

School of Physical and Chemical Sciences, North-West University, Hoffman Street Potchefstroom 2520, South Africa

## DATES:

Received: 06 May 2015

Revised: 31 July 2015

Accepted: 01 Aug. 2015

## KEYWORDS:

megacities; air pollution; photochemical box model; ozone; NOx

## HOW TO CITE:

Lourens ASM, Butler TM, Beukes JP, Van Zyl PG, Fourie GD, Lawrence MG. Investigating atmospheric photochemistry in the Johannesburg-Pretoria megacity using a box model. *S Afr J Sci.* 2016;112(1/2), Art. #2015-0169, 11 pages. <http://dx.doi.org/10.17159/sajs.2016/2015-0169>

© 2016. The Author(s).  
Published under a Creative Commons Attribution Licence.

Urban air pollution has become a major concern over the past decades. One of the largest conurbations in Sub-Saharan Africa is developed around the cities of Johannesburg and Pretoria (Jhb-Pta megacity). In this study, a photochemical box model with a detailed representation of ozone (O<sub>3</sub>) formation chemistry was used to investigate the state of current air quality and photochemical processes in the Jhb-Pta megacity, as well as scenarios that could possibly mitigate air pollution. Results indicated that the Jhb-Pta megacity is within a VOC-limited (or NOx-saturated) regime. Major sources of NOx include transport from the Mpumalanga Highveld and local traffic emissions. O<sub>3</sub> levels in the Jhb-Pta megacity will be more effectively reduced if VOC (volatile organic compound) emissions are decreased. A reduction of NOx emissions leads to an increase in O<sub>3</sub> because of a decrease in titration through the reaction with NO. The same effect was observed in various cities worldwide where O<sub>3</sub> levels increased when NOx emissions were reduced during emission control strategies. The effect of reducing vehicular emissions in the Jhb-Pta megacity on the production of O<sub>3</sub> was also investigated. A significant increase of approximately 23 ppb O<sub>3</sub> was observed when emissions of VOCs, NOx and CO were reduced by changing from Euro-0 to Euro-3 vehicles. It is therefore recommended that VOC emissions are decreased together with the implementation of Euro-3 and cleaner vehicles in the future.

## Introduction

One of the largest conurbations in Sub-Saharan Africa is developed around the cities of Johannesburg and Pretoria. This conurbation is one of the 40 largest metropolitan areas in the world with a population of over 10 million. Conurbations of this magnitude have been defined as megacities.<sup>1</sup> The Johannesburg-Pretoria (Jhb-Pta) megacity is also the central hub of economic activity in southern Africa. The main pollution sources in the Jhb-Pta megacity have been identified as traffic emissions, biomass and domestic combustion (space heating and cooking), as well as industrial activities.<sup>2,3</sup> The major pollutants emitted from these activities include nitrogen oxide (NO), nitrogen dioxide (NO<sub>2</sub>), sulphur dioxide (SO<sub>2</sub>), carbon monoxide (CO), particulate matter (PM) and various organic compounds. The Jhb-Pta megacity is also located relatively close to large industrialised regions in South Africa, i.e. the Mpumalanga Highveld, approximately 100 km to the west and the Vaal Triangle approximately 50 km to the south. It is therefore likely that air quality in the megacity will be influenced by the proximity of these areas.

According to the National Environmental Management Air Quality Act<sup>4</sup>, it is a requirement to utilise air quality models in decision-making processes and impact studies in South Africa. Implementation of this requirement has thus far mainly focused on applying dispersion modelling and not on improving processes within these models. However, these models are seldom developed and modified for the unique South African conditions, which differ vastly from conditions in America and/or Europe where most of these models were developed. Some of the dispersion models also include very limited chemical mechanisms.

Photochemical box models with a comprehensive chemical scheme are very useful tools to investigate air quality and the chemical processes within a region and are used to explore the main reactions that participate in O<sub>3</sub> (ozone) formation, as well as to assist in projecting the success of legislative air quality goals resulting from the implementation of emission control plans.<sup>5</sup> Since the first urban scale photochemical box model was successfully developed and used to assess air quality in urban areas,<sup>6</sup> various other photochemical models have been developed to study the production of O<sub>3</sub> in urban and rural areas.<sup>7-9</sup> Young and co-workers<sup>10</sup>, for example, developed and used a photochemical box model to investigate the best emission control strategy to reduce O<sub>3</sub> levels in Mexico City. Box models have also been applied in larger geographic regions.<sup>11-14</sup>

In an effort to investigate the interaction of O<sub>3</sub> precursor species and the resulting O<sub>3</sub> levels in the Jhb-Pta megacity, as well as to determine the possible contribution of O<sub>3</sub> precursor species emissions in areas surrounding the Jhb-Pta megacity, an existing photochemical box model, MECCA (Module Efficiently Calculating the Chemistry of the Atmosphere), was further developed and modified in this investigation. This modified version allowed a better representation of mixing of upwind air masses, and was termed MECCA-MCM-UPWIND. The MECCA-MCM-UPWIND model was used to perform sensitivity studies on the influence of different parameters on O<sub>3</sub> levels in the Jhb-Pta megacity. Possible scenarios to alter or mitigate pollution were also investigated.

## Model description

MECCA is a multi-purpose atmospheric chemistry model that contains chemical mechanisms describing tropospheric and stratospheric chemistry in both the gaseous and aqueous phases.<sup>15</sup> MECCA was originally developed by Sander et al.<sup>15</sup> at the Max-Planck Institute for Chemistry in Mainz, Germany. The full Master of Chemical Mechanism (MCM) was added to the MECCA box model and the MECCA-MCM model was used as described by Butler et al.<sup>16</sup> The MCM v3.1,<sup>17-18</sup> obtained via the website: <http://mcm.leeds.ac.uk/MCM>, is a near-explicit chemical mechanism that describes the detailed gas-phase chemical processes involved in the atmospheric degradation of a series of primarily emitted volatile organic compounds (VOCs). The existing photochemical

box model, MECCA-MCM, was further developed and improved in this study. This model was named MECCA-MCM-UPWIND, which included horizontal and vertical mixing processes, as well as boundary layer height variation. These processes were included to simulate the advection of upwind air masses into the modelling domain, as well as the entrainment from the troposphere through the diurnal mixing layer (ML) height variation, allowing a more detailed simulation of the processes controlling air quality in the Jhb-Pta conurbation.

## Model domain

The model domain was selected to be 100 km x 100 km, which included the Jhb-Pta megacity. The model domain is indicated by the rectangular block in the magnified area in Figure 1.

## Input data

Meteorological data, ML growth, pollutant emissions and pollutant mixing ratios were required as input data for the model. Five stations were identified within the modelling domain and one outside of it, from where data could be obtained. These stations are operated by the Department of Environmental Affairs, the City of Johannesburg and the City of Tshwane. The concentrations of additional species that were not measured at these monitoring stations at the time when data were collected were also required. A three month sampling campaign was therefore conducted from March to May in 2009 to obtain this additional information.<sup>3</sup> The limitations associated with using a three months data set collected during autumn were realised. There are significant differences in meteorological conditions experienced during different seasons. For example, winter has lower temperatures, greater diurnal variations and strong surface inversion layers prevailing in this part of South Africa leading to an increase in concentrations of pollutant atmospheric. However, the main objective for this sampling study was not to conduct a comprehensive measurement campaign, but rather to obtain representative data that could be used for the photochemical modelling. Previously published modelling studies have relied on even shorter measurement campaigns to obtain representative data.<sup>19-21</sup>

Only three of the five measurement stations located within the model domain conducted continuous meteorological measurements during the sampling period, because maintenance was being performed at the other two stations. Meteorological data obtained from these three measurement stations were averaged over a 3-month period (March–May) in 2009 to determine the diurnal variability of meteorological parameters in the Jhb-Pta megacity. According to these data, the average temperature,

atmospheric pressure, and relative humidity for autumn (March–May) in the Jhb-Pta megacity ranged from 12–22 °C, 84.3–84.6 kPa and 40–80%, respectively.

The mixing ratio input data required were the initial, tropospheric and upwind mixing ratios. The initial and tropospheric mixing ratios were obtained from ground-based measurements and published global model runs. The composition of the upwind mixing ratios, i.e. the air mass advected into the Jhb-Pta megacity, were determined by running the MECCA-MCM-UPWIND model with representative data for the Mpumalanga Highveld.

## Mixing layer height

The Air Pollution Model (TAPM) was utilised to simulate surface and free tropospheric meteorological data at a 2.5 km x 2.5 km resolution using synoptic scale meteorology (longitude/latitude grid at 1° grid spacing). The input data for TAPM were obtained from the US National Centre for Atmospheric Research. The average diurnal ML for three months (March–May) for the Jhb-Pta megacity was determined over a five consecutive year period (2004–2009) at a height of 1275 m.

## Emission Inventory

South Africa does not currently have a comprehensive gridded national inventory for sources of atmospheric emissions that are readily available to scientists. This complicated the acquisition of emission data used in the model. Detailed emission data do, however, exist for specific regions. These data sets were mostly obtained through research initiatives (e.g. SAFARI 2000), by metropolitan councils or by private companies on behalf of major industries. An emission inventory was developed for the Mpumalanga Highveld region during the Fund for the Research into Industrial Development Growth and Equity (FRIDGE) campaign in 2004.<sup>22</sup> Although this emission inventory was compiled for the Mpumalanga Highveld region, it also contained emission sources for the Jhb-Pta megacity. These emission sources included residential vehicles, industry, residential activities and biomass combustion as indicated in Table 1. Emissions for the species based on the FRIDGE studies were mainly used in this investigation. The FRIDGE emission inventory was also supplemented with the emission inventories developed for the Vaal Triangle during the Vaal Triangle Airshed Pollution Area (VTAPA) study in 2013<sup>23</sup> and the Gauteng study in 2009<sup>24</sup>, also presented in Table 1.

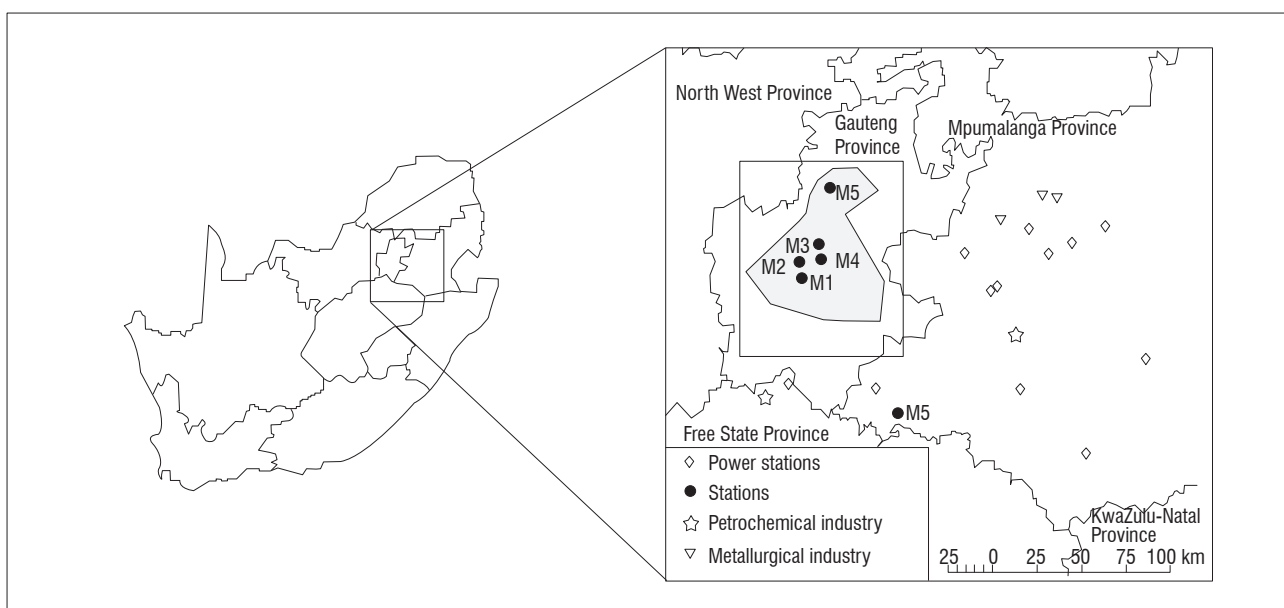


**Figure 1:** Model domain under investigation, with sampling stations in the Johannesburg-Pretoria (Jhb-Pta) megacity also shown. The Jhb-Pta megacity is indicated by the grey area.

**Table 1:** Emission sources (ton/year) for the Johannesburg-Pretoria megacity based on the Fund for the Research into Industrial Development Growth and Equity (FRIDGE)<sup>21</sup> emission inventory. The Vaal Triangle Airshed Pollution Area (VTAPA)<sup>22</sup> and Gauteng<sup>23</sup> studies are also included as supplementary data. It must also be noted that the use of Pb as an additive in petrol has been phased out since the FRIDGE emission inventory was established

Source types (ton/year)						
FRIDGE campaign						
Species	Vehicle sources	Industrial sources	Biomass burning	Residential/ Domestic fuel burning	Mines and Ash Dumps	Total
CO <sub>2</sub>	5 844 508		405 327	1 546 010		7 795 845
CO	272 579		10 33 122	90 232		362 811
CH <sub>4</sub>	1 211		24 348	3 327		28 886
Other NMHC	33 103			4 117		37 220
Benzene	484	3		139		626
Formaldehyde	292					292
Acetaldehyde	149			164		313
1,3 Butadiene	451					451
NO <sub>x</sub>	66 932	53 934		1 743		122 609
N <sub>2</sub> O						
SO <sub>2</sub>	10 103	20 811		7 877		38 791
Pb	242					242
N <sub>2</sub> O	200			39		239
VTAPA study						
SO <sub>2</sub>	448	247 224	84	826		
NO <sub>x</sub>	16 593	131 778	913	463		
PM <sub>10</sub>	1 068	13 668	1 494	1 836	4675	
Gauteng study						
SO <sub>2</sub>	15 718	23 050	291	13 151		74 850
NO <sub>x</sub>	127 311	108 002	1 505	1 492		264 777
PM <sub>10</sub>	4 663	9 550	2 427	3 796		23 051
Benzene	952	6		73		1 097
Formaldehyde	0.03	584				624
Acetaldehyde	0.06	298		12		332
1,3 Butadiene		906	80	9		1 055

The full MCM chemistry scheme in MECCA-MCM-UPWIND also included numerous non-methane hydrocarbon (NMHC) species. Although some studies have been published reporting BTEX (benzene, toluene, ethyl benzene and xylenes) for very limited sampling areas in South Africa,<sup>3,25</sup> no detailed speciated NMHC data existed for South Africa at the time of the study. Local inventories included benzene, formaldehyde, acetaldehyde and 1,3 butadiene as indicated in Table 1. Emission data (emission rates in molec/cm<sup>2</sup>/s) of NMHC species that were required as input data for the MECCA-MCM-UPWIND model were based on emission mass fractions for European conditions<sup>26</sup> and total carbon emissions (t/year) for Gauteng, which are listed in Table 2. As this was based on European conditions, the estimated NMHC emissions could potentially be an under- or over-estimate.

### Diurnal variation of traffic emissions

In the Jhb-Pta megacity, traffic is regarded as the major emission source, contributing to approximately 80% of the total nitrogen oxide (NO<sub>x</sub>) emissions.<sup>27</sup> Vehicles also account for approximately 60% of benzene, 100% of formaldehyde, 99% of acetaldehyde and 70% of the total NMHC emissions.<sup>28</sup> Pollutant species from traffic emissions have a significant diurnal variability. Goyns<sup>29</sup> determined the real-world fuel consumption and emissions from passenger vehicles for Johannesburg from 2001 to 2005. According to Goyns<sup>29</sup>, most of the vehicular emissions are emitted during the peak traffic hour periods 06:00–09:00 and 16:00–18:30. The above-mentioned diurnal variability is in general agreement with Menut et al.<sup>30</sup> (Schaberg. 2012. Written communication April 23), who derived averaged hourly emission factors (Figure 2) based on pollutant concentrations

in various cities in Europe by utilising the chemistry transport model CHIMERE. As hourly values were needed for the photochemical box model used in this study, pollutant species were incorporated as hourly emissions in the model, based on the emission factors presented in Figure 2.

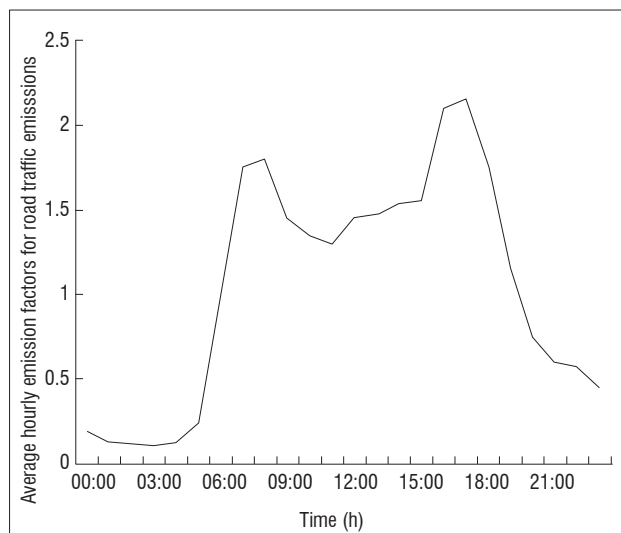


**Figure 2:** Diurnal variation of traffic emissions based on factor estimation (adopted from Menut et al.<sup>28</sup>).

Total atmospheric NO and NO<sub>2</sub> concentrations are commonly measured together as NO<sub>x</sub> concentrations. For the model, however, it was required that the emissions of NO and NO<sub>2</sub> species were separated. Various factors influence the NO/NO<sub>2</sub> ratio from raw exhaust gas, e.g. petrol or diesel engines, or exhaust gas from diesel engines after processing by a catalytic converter.<sup>31</sup> The NO<sub>2</sub> fraction in NO<sub>x</sub> varies between 5% and 25% by mass, depending on the type of vehicle and fuel.<sup>31</sup> The European Monitoring and Evaluation Programme (EMEP) of the European Environmental Agency (EAA) compiled an air pollution emission inventory guidebook (EMEP/EEA), which provides guidance on estimating emissions from both anthropogenic or natural emission sources.<sup>32</sup> Based on the EMEP/EEA guidebook, it was assumed in the model that the NO/NO<sub>2</sub> ratio for raw exhaust gas vehicle emissions was 80% NO and 20% mass fraction NO<sub>2</sub>.

The Euro fuel specification is defined as the acceptable limits for exhaust emissions of new vehicles in Europe in order to meet their stringent emission regulations. The 'criteria' atmospheric pollutants are regulated through these standards. South Africa has also adopted this standard classification reference method. The different Euro specifications are an indication of when they came into force, i.e. Euro-0, pre-1993; Euro-1 in 1993; Euro-2 in 1996; Euro-3 in 2000, Euro-4 in 2005 and Euro-6 in 2014. According to Goyns<sup>29</sup>, the private passenger vehicle fleet in the Jhb-Pta megacity from 2001 to 2005 consisted of approximately 45% Euro-0 type petrol vehicles, 10% Euro-2 diesel vehicles, 30% Euro-2 petrol vehicles and 15% Euro-3 petrol vehicles. The percentages of each pollutant species emitted from the different Euro classified vehicles that was used in this study are listed in Table 3.

**Table 2:** NMHC (non-methane hydrocarbon) emissions (ton/year) based on the mass fraction (adopted from Derwent et al.<sup>24</sup>)

Species	Name	ton/year	Species	Name	ton/year
Isobutene1-butene	C <sub>4</sub> H <sub>10</sub>	151	Butane	C <sub>4</sub> H <sub>10</sub>	1312
mp-Xylene	C <sub>8</sub> H <sub>10</sub>	939	trans-2-Butene	C <sub>4</sub> H <sub>8</sub>	288
o-Xylene	C <sub>8</sub> H <sub>10</sub>	813	cis-2-Butene	C <sub>4</sub> H <sub>8</sub>	288
1,2,3-Trimethyl-benzene	C <sub>9</sub> H <sub>12</sub>	166	1-Pentene	C <sub>5</sub> H <sub>10</sub>	99
Acetone	C <sub>3</sub> H <sub>6</sub> O	785	n-Pentane	C <sub>5</sub> H <sub>12</sub>	634
Ethanol	C <sub>2</sub> H <sub>6</sub> O	4474	Isoprene	C <sub>5</sub> H <sub>8</sub>	1
Ethylene	C <sub>2</sub> H <sub>4</sub>	1168	2-Methyl-2-butene	C <sub>5</sub> H <sub>10</sub>	83
Toluene	C <sub>7</sub> H <sub>8</sub>	2149	n-Hexane	C <sub>6</sub> H <sub>14</sub>	420
Propylene	C <sub>3</sub> H <sub>6</sub>	50	2-Methyl-heptane	C <sub>6</sub> H <sub>18</sub>	498
Propane	C <sub>3</sub> H <sub>8</sub>	164	Cyclohexane	C <sub>6</sub> H <sub>12</sub>	1
Isobutene	C <sub>4</sub> H <sub>10</sub>	1312	2-Methyl-hexane	C <sub>7</sub> H <sub>16</sub>	167
n-Octane	C <sub>8</sub> H <sub>18</sub>	89	n-Heptane	C <sub>7</sub> H <sub>16</sub>	108
Ethyl-benzene	C <sub>8</sub> H <sub>10</sub>	409			

**Table 3:** Input data for the Johannesburg-Pretoria (Jhb-Pta) megacity model run

Euro-0 petrol (42% of total Jhb-Pta megacity passenger fleet)	Euro-2 diesel (10% of total Jhb-Pta megacity passenger fleet)	Euro-2 petrol (30% of total Jhb-Pta megacity passenger fleet)	Euro-3 petrol (15% of total Jhb-Pta megacity passenger fleet)
40% CO <sub>2</sub>	19% CO <sub>2</sub>	27% CO <sub>2</sub>	15% CO <sub>2</sub>
88% CO		10% CO	2% CO
93% HC		5% HC	0.5% HC
82% NO <sub>x</sub>	14% NO <sub>x</sub>	3% NO <sub>x</sub>	0.4% NO <sub>x</sub>

**Table 4:** Vehicle emissions for Johannesburg-Pretoria megacity according to the Euro classification<sup>29</sup>

Species	Formula	Initial mixing ratio (ppb)	Tropospheric mixing ratio (ppb)	Upwind mixing ratio (ppb) from Upwind model run	Emissions (molec/cm <sup>2</sup> /s)
Nitrogen monoxide	NO	20	0.1	40	1.2x10 <sup>11†</sup>
Nitrogen dioxide	NO <sub>2</sub>	14	1	38	1.0x10 <sup>10†</sup>
Peroxyacetyl nitrate	PAN	2	0.02	0.85	-
Ozone	O <sub>3</sub>	7	65	19	-
Carbon monoxide	CO	2700	75	2982	9.1x10 <sup>12†</sup>
Carbon dioxide	CO <sub>2</sub>		345 <sup>‡</sup>		6.7x10 <sup>11</sup>
Methane	CH <sub>4</sub>	1800	175 <sup>‡</sup>	6260	1.2x10 <sup>11</sup>
Ethane	C <sub>2</sub> H <sub>6</sub>		0.4	5.8	12.1x10 <sup>8</sup>
Ethylene	C <sub>2</sub> H <sub>4</sub>				1.7x10 <sup>9†</sup>
Formaldehyde	CH <sub>2</sub> O				6.6x10 <sup>8†</sup>
Propylene	C <sub>3</sub> H <sub>6</sub>				1.4x10 <sup>9†</sup>
Propane	C <sub>3</sub> H <sub>8</sub>			0.64	1.3x10 <sup>9†</sup>
Isobutene 1-butene	C <sub>4</sub> H <sub>10</sub>				5.4x10 <sup>8†</sup>
Butane	C <sub>4</sub> H <sub>10</sub>				1.9x10 <sup>9†</sup>
Trans-2-Butene	C <sub>4</sub> H <sub>8</sub>				4.3x10 <sup>8†</sup>
Cis-2-Butene	C <sub>4</sub> H <sub>8</sub>				4.3x10 <sup>8†</sup>
1-pentene	C <sub>5</sub> H <sub>10</sub>				1.2x10 <sup>8†</sup>
N-Pentane	C <sub>5</sub> H <sub>12</sub>				7.7x10 <sup>8†</sup>
2-Methyl-2-butene	C <sub>5</sub> H <sub>10</sub>				1.0x10 <sup>8†</sup>
N-Hexane	C <sub>6</sub> H <sub>14</sub>				5.8x10 <sup>8†</sup>
Benzene	C <sub>6</sub> H <sub>6</sub>	3	0.01 <sup>†</sup>	0.62	5.5x10 <sup>8†</sup>
Cyclohexane	C <sub>6</sub> H <sub>12</sub>				4.9x10 <sup>5†</sup>
2-Methyl-hexane	C <sub>7</sub> H <sub>16</sub>				1.4x10 <sup>8†</sup>
N-Heptane	C <sub>7</sub> H <sub>16</sub>				9.3x10 <sup>7†</sup>
Toluene	C <sub>7</sub> H <sub>8</sub>	3	0.01	0.8	9.8x10 <sup>8†</sup>
2-Methyl-heptane	C <sub>8</sub> H <sub>18</sub>				3.7x10 <sup>8†</sup>
N-Octane	C <sub>8</sub> H <sub>18</sub>				6.7x10 <sup>7†</sup>
Ethyl-benzene	C <sub>8</sub> H <sub>10</sub>	4	0.01	0.23	2.7x10 <sup>8†</sup>
Mp-Xylenes	C <sub>8</sub> H <sub>10</sub>	4	0.01	0.42	9.9x10 <sup>7†</sup>
O-Xylene	C <sub>8</sub> H <sub>10</sub>	4	0.01	0.41	2.4x10 <sup>8†</sup>
1,2,3-Trimethyl-benzene	C <sub>9</sub> H <sub>12</sub>				9.8x10 <sup>8†</sup>
Acetone	C <sub>3</sub> H <sub>6</sub> O				7.0x10 <sup>12†</sup>
Acetylene	C <sub>2</sub> H <sub>2</sub>		0.04		1.9x10 <sup>10†</sup>
Ethanol	C <sub>2</sub> H <sub>6</sub> O				4.0x10 <sup>9†</sup>
1,3-butaine	C <sub>4</sub> H <sub>6</sub>				1.0x10 <sup>8†</sup>

<sup>†</sup> Emissions emitted hourly in the model. Listed values present the emission at the start of the model run.

<sup>‡</sup> Mixing ratio in part per million (ppm)

As indicated in Table 3, Euro-0 petrol vehicles have the highest emissions and produce 40% CO<sub>2</sub>, 88% CO, 93% hydrocarbon (HC) and 82% NO<sub>x</sub> emissions, whereas Euro-3 petrol vehicles contribute much less, with 15% CO<sub>2</sub>, 2% CO, 0.5% HC and 0.4% NO<sub>x</sub> emissions. These derived emissions excluded heavy-duty vehicles and minibus taxis, which also contribute significantly to vehicular emissions in the Jhb-Pta megacity. In this study, the worst case scenario was assumed in the model base case run, i.e. that all vehicles in the Jhb-Pta megacity were Euro-0 type. During the sensitivity analysis, the impact of the conversion of all vehicles to Euro-3 type on pollutant species in the atmosphere was also investigated.

### Initial and tropospheric mixing ratios

The averaged initial mixing ratios of most of the criteria pollutants (NO, NO<sub>2</sub>, O<sub>3</sub> and BTEX) were obtained from data collected at the stations indicated in Figure 1, from literature,<sup>15,33,34</sup> as well as from data collected during a three-month (March–May 2010) monitoring campaign.<sup>3</sup> These average initial mixing ratios are listed in Table 4. Measurements conducted at midnight (00:00) were used as the initial mixing ratio values in the MECCA-MCM-UPWIND model run, because the start time of the model is 00:00.

No data were available for most of the species in the Jhb-Pta megacity as a function of height above ground level within the troposphere and therefore these mixing ratios were estimated, either through model simulations or obtained from literature. Estimated tropospheric mixing ratios for species were obtained from the global chemistry-climate model (EMAC).<sup>15</sup> Output files from EMAC were generated for each day for all the major pollutant species (i.e. CO, CH<sub>4</sub>, PAN, NO, NO<sub>2</sub>, SO<sub>2</sub>) and used as input into the MECCA-MCM-UPWIND model. With the exception of CO and CH<sub>4</sub>, the other most important tropospheric organic trace gases are ethane (C<sub>2</sub>H<sub>6</sub>) and ethyne (C<sub>2</sub>H<sub>2</sub>).<sup>15,33</sup> C<sub>2</sub>H<sub>6</sub> is the second most abundant HC in the atmosphere and has a lifetime of approximately two months,<sup>35</sup> whereas C<sub>2</sub>H<sub>2</sub> has an estimated lifetime of 2–4 weeks in the atmosphere.<sup>36</sup> No data were available for these species in the Jhb-Pta megacity, so the global mixing ratios in the southern hemisphere of 0.04 ppb and 0.044 ppb for C<sub>2</sub>H<sub>6</sub> and C<sub>2</sub>H<sub>2</sub>, respectively, were used.<sup>32</sup> The global mixing ratios for CO<sub>2</sub>, CO and CH<sub>4</sub> were also used.<sup>37</sup> Most vertical tropospheric O<sub>3</sub> profiling studies in southern Africa have been conducted during sampling campaigns, e.g. SAFARI 2000. Vertical tropospheric O<sub>3</sub> measured at Irene (Pretoria) was reported to be 60–65 ppb, between 2 km and 2.5 km above ground level.<sup>38,39</sup> Concentrations of species such as O<sub>2</sub>, N<sub>2</sub> and CO<sub>2</sub> were fixed throughout the model runs.

### Upwind mixing ratios

This study also includes a representation of advection of air masses from the highly polluted Mpumalanga Highveld into the Jhb-Pta megacity because of its proximity to the Jhb-Pta megacity. The composition of the air masses entering the Jhb-Pta megacity was simulated using MECCA-MCM-UPWIND making use of input data representative of the Mpumalanga Highveld. A total of 5 air quality monitoring stations within the Mpumalanga Highveld were used to obtain initial mixing ratios for this model run.<sup>3</sup> The average wind speed used was 1.7 m/s as determined at four of these air quality monitoring stations. Model spin-up time of 24 h was performed in order to provide realistic initial concentrations for the second 24 h. The model results averaged over the second 24 h period were used as the upwind mixing ratio inputs for the Jhb-Pta megacity base-case and sensitivity runs. The same ML height utilised for the Jhb-Pta megacity was used for this model run, as the Mpumalanga Highveld is situated at approximately the same height above sea level. Recently Korhonen et al.<sup>40</sup> also indicated that the ML over the Mpumalanga Highveld and Jhb-Pta are similar.

Industrial activities are the main emission sources in the Mpumalanga Highveld. These industries mostly operate 24 h per day, so there is no diurnal variability in the emissions.<sup>41</sup> Therefore it was not necessary to specify a temporal profile of emissions in the model run. Emission data for the Mpumalanga Highveld obtained from the FRIDGE study were utilised.

According to literature, the initial NO/NO<sub>2</sub> ratio on release from a coal-fired power station into the atmosphere is about 95/5 by mass, while

the release from vehicles is 80/20 by mass. However, traffic emissions in the Mpumalanga Highveld are much lower compared to industrial emissions. Therefore, the assumption to use the ratio of NO/NO<sub>2</sub> from the Highveld as 95% NO and 5% mass fraction NO<sub>2</sub> was made.<sup>42</sup>

The mixing ratios of all the pollutant species measured at the air quality monitoring stations in the Mpumalanga Highveld were used as initial mixing ratios for the Highveld model run. Average diurnal concentrations for the three months (March–May) were used. For this model run, the upwind mixing of species in the Mpumalanga Highveld was not included as the simulation focussed on the aging of air mass transported between the Mpumalanga Highveld and the Jhb-Pta megacity. Therefore, the upwind mixing ratio of the species within the Mpumalanga Highveld was the same as the initial mixing ratios for all the simulations. The result from this Mpumalanga Highveld model run, which was used as input for the Jhb-Pta megacity, are summarised in Table 4.

## Results and Discussion

### Base case run

A base case model run using the input data, as previously discussed, was used to compare predicted pollutant mixing ratios to measured mixing ratios obtained during the sample campaign. The averaged wind speed of 1.7 m/s based on the metrological data was used in the Jhb-Pta model runs. Figure 3 presents the comparison between the measured and modelled results for NO, NO<sub>2</sub> and O<sub>3</sub> mixing ratios.

The modelled diurnal NO pattern was in general in good agreement with the measured NO. The diurnal variation in the modelled NO can be attributed to changes in emissions, transport, chemistry and the ML height in the box defined for the model. The peak of NO in the morning and evening was well reproduced by MECCA-MCM-UPWIND. This increased NO mixing ratio can be ascribed to increased emissions within the model. The measured data also showed the same tendency with NO usually peaking in the morning because of increases in emissions from vehicles and household combustion, in conjunction with a relatively low boundary layer height. The early morning peak between 6:00 and 9:00 coincided with the time that commuters travel to work.<sup>3</sup> The second peak observed between 16:00 and 21:00 for both the measured and modelled data can be attributed to traffic emissions and household combustion (space heating and cooking).<sup>43</sup> A decrease in NO emissions was observed for the measured data after 19:00. This is the result of a significant decrease in NO sources. However, the model results indicated an increase in NO mixing ratios. This can be explained by emission and ML effects in the model. When the ML decreases within the model, it stops the vertical mixing from above the ML, which results in the accumulation of NO because of the decrease in volume and emissions emitted into the model.

It seems that the modelled NO<sub>2</sub> mixing ratios were somewhat over-predicted by MECCA-MCM-UPWIND, although it was in relatively good agreement with the diurnal variability determined with the measured NO<sub>2</sub> concentrations. Because 20% of NO<sub>x</sub> emitted from vehicles are NO<sub>2</sub>, diurnal changes of traffic emissions will also influence the trend observed. The first NO<sub>2</sub> peak can be explained by the increased traffic emissions resulting in higher NO<sub>2</sub> mixing ratios and decrease as the ML height increases, which results in NO and NO<sub>2</sub> mixing ratios decreasing, which implies that less NO is available to chemically transform to NO<sub>2</sub>. This leads to a decrease in NO<sub>2</sub> mixing ratios. The second observed peak later in the day can be related to the slowed photolysis rate of NO<sub>2</sub>, resulting in the accumulation of NO<sub>2</sub>.

The diurnal cycle of O<sub>3</sub> was well predicted by MECCA-MCM-UPWIND and is in good agreement with measured concentrations, although some differences between the measured and modelled data were observed. MECCA-MCM-UPWIND simulated very low mixing ratios of O<sub>3</sub> during the early morning hours and evening hours with a slight over-prediction during the daytime mixing ratio of O<sub>3</sub>. O<sub>3</sub> is accumulated through photochemical oxidation processes throughout the day until dusk. At this time, the photochemical processes slow down because of to the lower levels of solar radiation. The ML height decrease also results in no entrainment from above. The almost zero O<sub>3</sub> levels during night-time for the model run can be attributed to the NO<sub>x</sub>-titration effect within the model.

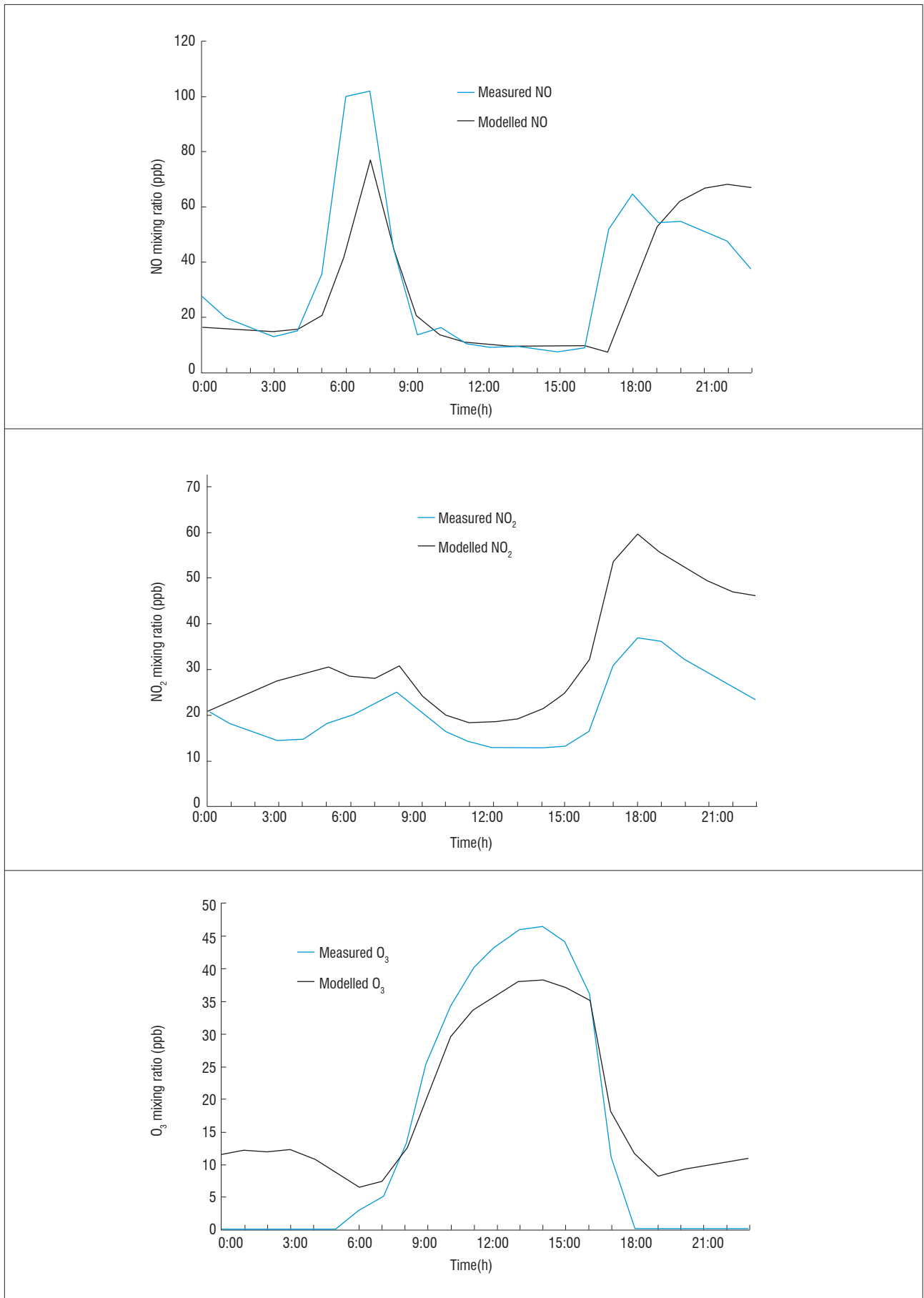


Figure 3: Modelled and measured diurnal mixing ratios for NO, NO<sub>2</sub> and O<sub>3</sub>.

Model results presented later in the paper (Figure 5) indicate that there is enough NO in the model to completely convert all the O<sub>3</sub> to NO<sub>2</sub>. NOx titration can drive O<sub>3</sub> concentrations in urban areas to less than 1 ppb.<sup>44</sup> The discrepancy between the measured and modelled results can be considered as a possible limitation of the model. However, other modelling studies, e.g. Stockwell et al.<sup>45</sup>, have emphasised the difficulty of correctly representing night-time chemistry in models.

#### Sensitivity of O<sub>3</sub> production to changes in wind speed

In this model run, the sensitivity of the Jhb-Pta megacity to the rate at which external pollution is advected into the megacity was examined. Although O<sub>3</sub> concentrations in the atmosphere are influenced by changes in meteorological conditions, such as ML height, temperature and wind speed, in this scenario only wind speed was varied. The influence of no wind (0 m/s), medium wind speed (1.7 m/s) and high wind speed

(3.4 m/s) from the Mpumalanga Highveld was calculated with the MECCA-MCM-UPWIND model. The results presented in Figure 4 indicate that lower wind speeds lead to increases in O<sub>3</sub> mixing ratios in the Jhb-Pta megacity. The results show that wind speed plays an important role in the processes that control O<sub>3</sub> concentrations in the atmosphere. According to the model, O<sub>3</sub> levels are 12 ppb higher when there is no wind present compared to medium wind speed, while O<sub>3</sub> mixing ratios are 22 ppb lower during medium wind speed conditions compared to higher wind speeds.

When the upwind air mass enters the Jhb-Pta megacity, it is instantaneously mixed in the model with the air in the Jhb-Pta megacity. This implies that if the wind speed doubles and other conditions remain equal, more NOx is transported from the Mpumalanga Highveld into the model, which can lead to the titration of O<sub>3</sub> within the Jhb-Pta megacity as is evident from Figure 5.

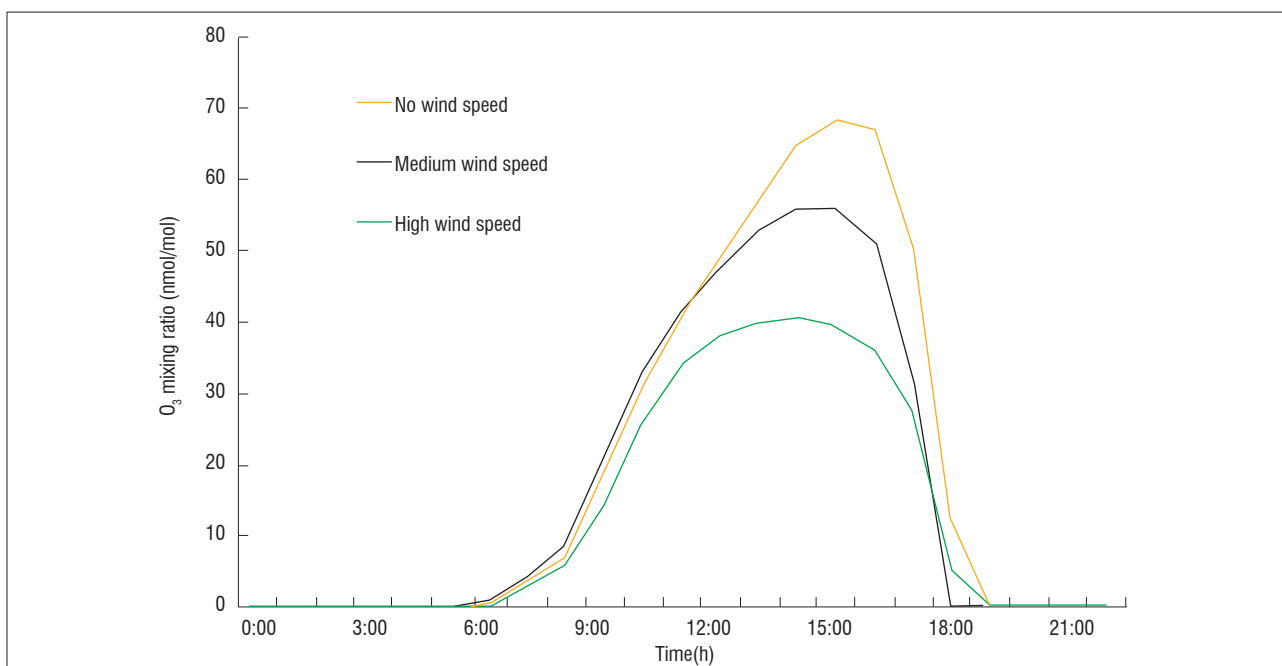


Figure 4: Sensitivity of the model to O<sub>3</sub> mixing ratios with changes in wind speed.

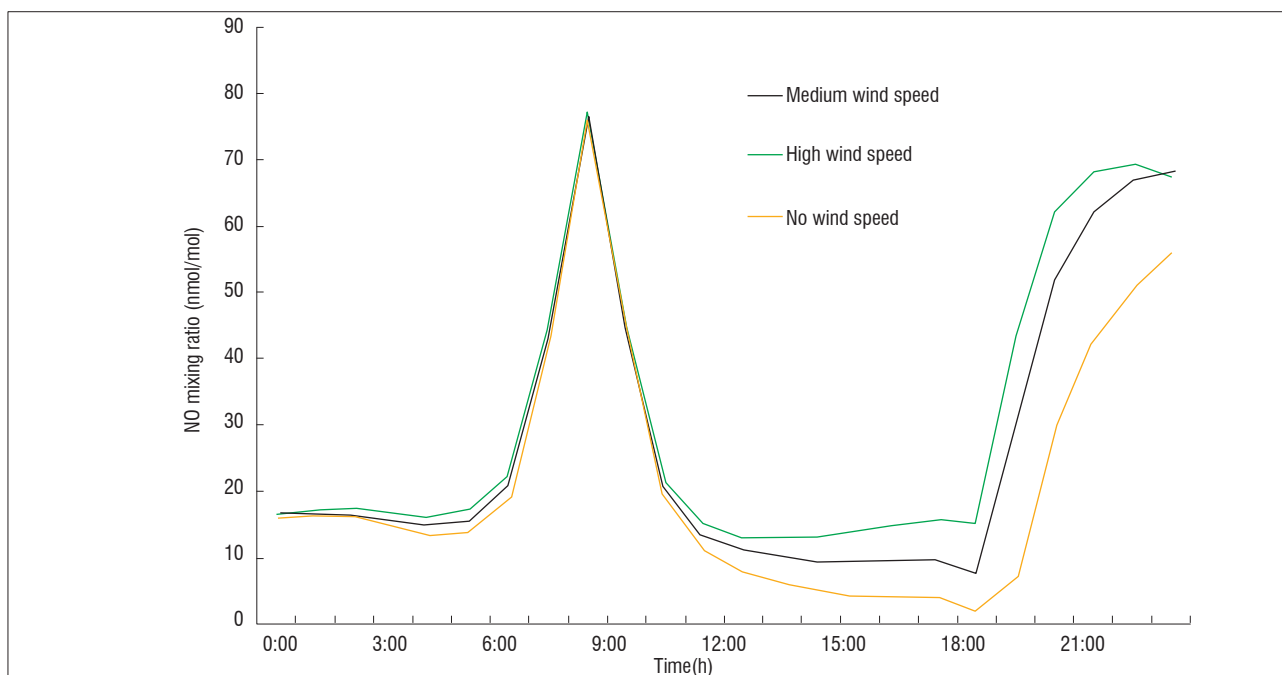
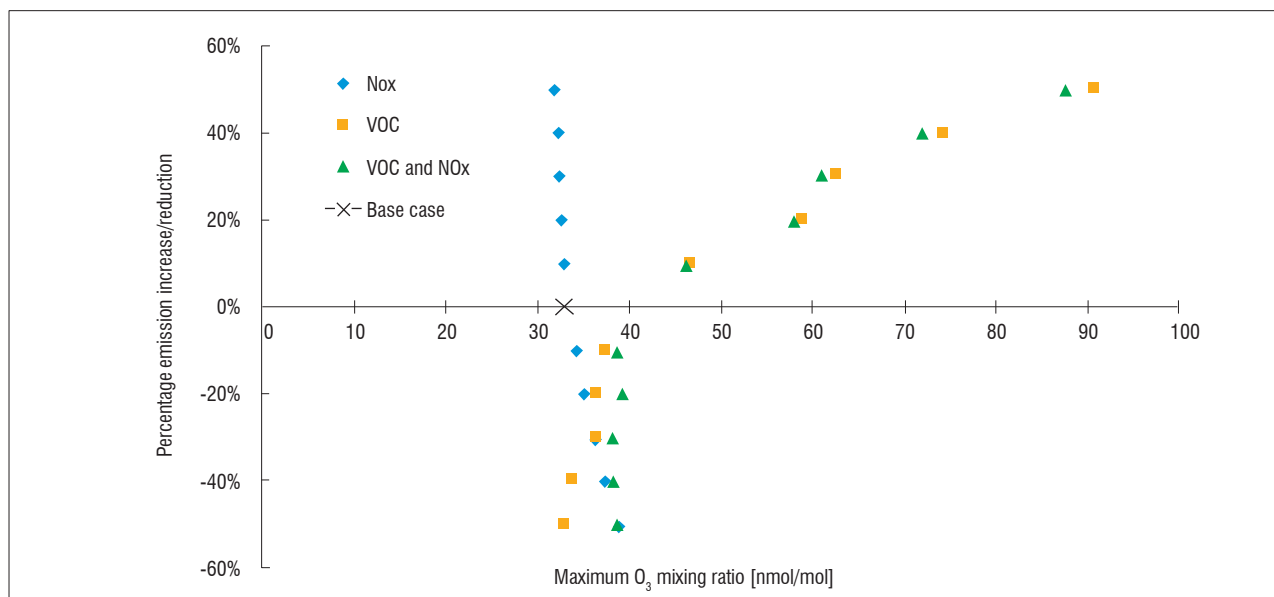
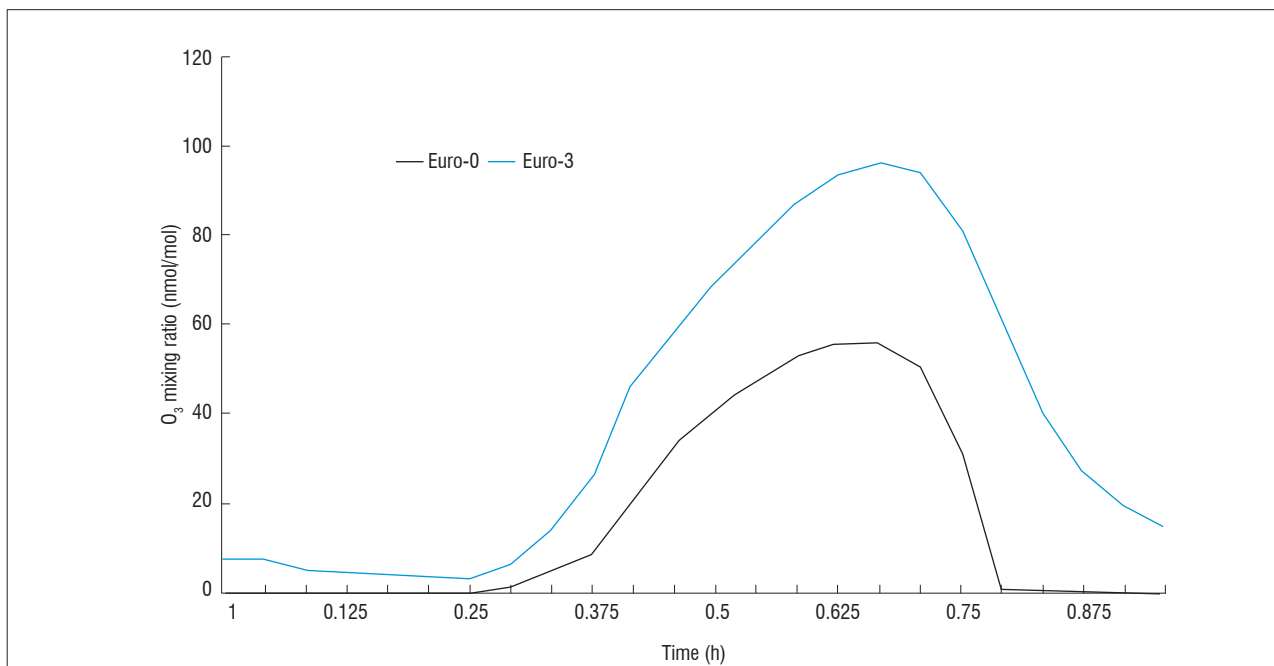


Figure 5: Sensitivity of the model to NO mixing ratios with changes in wind speed.



**Figure 6:** The change in the maximum  $O_3$  mixing ratios associated with each percentage increase/decrease of NOx and VOCs (volatile organic compounds) emissions.



**Figure 7:** Comparison of  $O_3$  production in the Johannesburg-Pretoria megacity by changing from Euro-0 to Euro-3 classified vehicles.

Lower wind speeds implicate longer reaction times, assuming all other conditions stay the same. Additionally,  $O_3$  is a secondary pollutant whose concentration will increase with time as the precursor species react. It is evident from Figure 5 that NO levels increase at higher wind speeds from the Mpumalanga Highveld. The same effect was observed for  $O_3$ . When a lower concentration of  $O_3$  is advected into the Jhb-Pta megacity at twice the rate, the concentrations of  $O_3$  within the Jhb-Pta megacity will decrease. Increasing the  $O_3$ -titration effect results in decreased  $O_3$  levels in the Jhb-Pta megacity. In stagnant conditions where no upwind air is advected into the Jhb-Pta megacity, the concentration of the pollutants in the Jhb-Pta megacity is only influenced by the initial concentrations, emission levels, vertical mixing and chemistry within the megacity. Under these conditions, the local emissions and vertical mixing tend to contribute significantly to the photochemistry for the formation of  $O_3$ .

### Sensitivity of $O_3$ production to changes in Jhb-Pta megacity emissions

In order to calculate the effect of emissions of VOCs and NOx in the Jhb-Pta megacity on the photochemical production of  $O_3$  occurring within the megacity, six case studies were conducted. These case studies were conducted for the reduction and increase in VOC and NOx concentrations separately, as well as in conjunction with each other. In order to avoid potential nonlinearities associated with changing the chemical regime (e.g. NOx-limited or VOC-limited), increments of 10–50% were used. The maximum  $O_3$  mixing ratio resulting from the percentage change for each case study was plotted (Figure 6). The  $O_3$  base case concentration is indicated by the black cross at 56 ppb.

The relationship between NO<sub>x</sub> and VOC concentrations for the production of O<sub>3</sub> can be illustrated by means of isopleth plots.<sup>46</sup> On these isopleth plots, certain chemical regimes can be identified, i.e. areas where O<sub>3</sub> formation depends either on NO<sub>x</sub> or VOC concentrations. The results obtained from the incremental changes in Figure 6 can be related to these O<sub>3</sub> isopleth plots. An increase in O<sub>3</sub> production is observed when VOC emissions are increased, while O<sub>3</sub> levels decrease when NO<sub>x</sub> emissions are increased. Reducing NO<sub>x</sub> emissions while keeping VOC emissions constant will therefore result in an increase in O<sub>3</sub> concentrations. The changes of O<sub>3</sub> mixing ratios resulting from the increase in NO<sub>x</sub> emissions are lower than the increase of O<sub>3</sub> levels observed when NO<sub>x</sub> emissions are reduced. The changes observed with the model can be related to the isopleths in the VOC-sensitive regime. Chemically, this observation can be explained by the reaction of the HO• radical with NO<sub>2</sub> producing HNO<sub>3</sub> that is dominant at high concentrations of NO<sub>x</sub> and suppresses the concentration of the HO• radical. The production of HO<sub>2</sub>• and RO<sub>2</sub>• radicals, which are produced by the oxidation of VOCs with HO• radicals, is slowed down and results in less O<sub>3</sub> production. Regarding the O<sub>3</sub> isopleths, the results shown in Figure 6 indicate that the Jhb-Pta megacity is a VOC-limited (or NO<sub>x</sub>-saturated) regime. Therefore, according to the model, O<sub>3</sub> production in the Jhb-Pta megacity will be reduced most significantly when the VOC emissions in Jhb-Pta megacity are reduced.

#### Effect of vehicle fleet emissions on O<sub>3</sub> production

The fuel strategy of the South African government is to only have vehicles on the roads classified as Euro-4 and higher emissions standards in the future.<sup>47</sup> Therefore, in this case study, the effect of reducing vehicular emissions in the Jhb-Pta megacity on the production of O<sub>3</sub> was also investigated. Based on the values of emissions associated with each Euro-classified vehicle listed in Table 3, a model sensitivity run was performed in which emissions of VOCs, NO<sub>x</sub> and CO were reduced from Euro-0 to Euro-3 vehicles. The results are presented in Figure 7. As is evident, a significant increase in O<sub>3</sub> production of approximately 23 ppb is observed. This is consistent with other modelled sensitivity studies of traffic emissions that also predict that future urban O<sub>3</sub> concentrations will increase in many cities by 2050 because of the reduction in NO<sub>x</sub> titration of O<sub>3</sub>, despite the implementation of O<sub>3</sub> control regulations.<sup>48</sup> The increase of O<sub>3</sub> is also consistent with the NO<sub>x</sub> saturated regime as indicated in Figure 6, which indicated that VOCs should be reduced concurrently with NO<sub>x</sub> in order to avoid the increase in O<sub>3</sub> levels.

## Conclusions

Compared to measured data, MECCA-MCM-UPWIND was able to predict the diurnal variability of NO, NO<sub>2</sub> and O<sub>3</sub> within the Jhb-Pta megacity relatively well. Daytime chemistry was especially well simulated, while small under-predictions were calculated for night-time chemistry. Some of the uncertainties in the model can possibly be attributed to the emission inventories utilised and the deficiency of well-defined NMHC data for the Jhb-Pta megacity.

Sensitivity analyses showed that O<sub>3</sub> mixing ratios decreased with increasing wind speed and increased with decreasing wind speed within the Jhb-Pta megacity. This indicated that the Mpumalanga Highveld could potentially be a major source of NO<sub>x</sub> in the Jhb-Pta megacity. This implies that if the air quality for the larger surrounding area improves, the concentration of the secondary pollutant O<sub>3</sub> will increase in the Jhb-Pta megacity.

The influence of NO<sub>x</sub> and VOC concentrations on O<sub>3</sub> formation in the Jhb-Pta megacity indicated that the Jhb-Pta megacity is a VOC-limited (or NO<sub>x</sub>-saturated) regime. Therefore, O<sub>3</sub> levels in the Jhb-Pta megacity will be more effectively reduced if VOC emissions decrease. A reduction of NO<sub>x</sub> emissions will lead to an increase in O<sub>3</sub> because of a decrease in titration through the reaction with NO. The same effect was observed in various cities worldwide where O<sub>3</sub> levels increased when NO<sub>x</sub> emissions were reduced during emission control strategies. The increase of O<sub>3</sub> can be avoided if VOCs are also reduced.

The effect of reducing vehicular emissions in the Jhb-Pta megacity on the instantaneous production of O<sub>3</sub> was also investigated. A significant increase of approximately 23 ppb O<sub>3</sub> production was observed when

emissions of VOCs, NO<sub>x</sub> and CO were reduced from Euro-0 to Euro-3 vehicles. This is consistent with other modelled sensitivity studies of traffic emissions, which also predict that future urban O<sub>3</sub> concentrations will increase in many cities by 2050 as a result of the reduction in NO<sub>x</sub> titration of O<sub>3</sub>, despite the implementation of O<sub>3</sub> control regulations.

The limitation associated with comparison of the modelled data with a three month measured data set was realised. It is recommended in future that modelled data be compared to a complete 1-year ground measurement data set, which will account for different meteorological conditions occurring in each of the seasons. Future work should also aim at improving the model to reduce over- and under-prediction of concentrations of species. Expanded and accurate emission inventories for South Africa will be pivotal in improving modelled data sets. It is also important that changes in the vehicular fleet should be reflected in improved emission inventories.

## Acknowledgments

The authors acknowledge Sasol Research & Development and the National Research Foundation for their financial support.

## Authors' contributions

A.S.M.L., T.M.B., J.P.B. and P.G.v.Z. were the main investigators in this study. A.S.M.L., T.M.B., J.P.B. and P.G.v.Z. were project leaders of the study and wrote the manuscript. A.S.M.L. conducted this study as part of her PhD and performed most of the experimental work. P.G.v.Z. and J.P.B. were also study leaders of this PhD study, while T.M.B. was an assistant study leader. G.D.F. and M.G.L. made conceptual and logistical contributions.

## References

1. Molina MJ, Molina LT. Megacities and atmospheric pollution. *J Air Wast Manage.* 2004;54:644–680. <http://dx.doi.org/10.1080/10473289.2004.10470936>
2. Lourens ASM, Beukes JP, Van Zyl PG, Fourie GD, Burger JW, Pienaar JJ, et al. Spatial and temporal assessment of gaseous pollutants in the Mpumalanga Highveld of South Africa. *S Afr J Sci.* 2011;107(1/2) Art. #269, 8 pages. <http://dx.doi.org/10.4102/sajs.v107i1/2.269>
3. Lourens ASM, Butler TM, Beukes JP, Van Zyl PG, Beirle S, Wagner T, et al. Re-evaluating the NO<sub>2</sub> hotspot over the South African Highveld. *S Afr J Sci.* 2012;108(11/12) Art. #1146, 6 pages. <http://dx.doi.org/10.4102/sajs.v108i11/12.1146>
4. National Environmental Management: Air Quality Act No. 39 of 2004 section 63. *Government Gazette.* 2005 Feb 24; Vol. 476, No. 27318. Available from: [https://www.environment.gov.za/sites/default/files/legislations/nema\\_amendment\\_act39.pdf](https://www.environment.gov.za/sites/default/files/legislations/nema_amendment_act39.pdf)
5. Jin S, Demerjian KL. A photochemical box model for urban air quality study. *Atmos Environ.* 1993;278(1):371–387. [http://dx.doi.org/10.1016/0957-1272\(93\)90015-X](http://dx.doi.org/10.1016/0957-1272(93)90015-X)
6. Schere KL, Demerjian KL. User guide for the photochemical box model (PBM). Research Triangle Park, NC: Environmental Sciences Research Laboratory; 1984.
7. Butler TM, Lawrence MG, Taraborrelli D, Lelieveld J. Tagged ozone production potential (TOPP) of volatile organic compounds. *Atmos Environ.* 2011;45:4082–4090. <http://dx.doi.org/10.1016/j.atmosenv.2011.03.040>
8. Kleinman LI. Seasonal dependence of boundary layer peroxide concentration: The low and high NO<sub>x</sub> regimes. *J Geophys Res.* 1991;96:20721–20733. <http://dx.doi.org/10.1029/91JD02040>
9. Sillman S. New developments in understanding the relation between ozone, NO<sub>x</sub> and hydrocarbons in urban atmosphere. *Adv S Phys Chem.* 1995;3:145–171. [http://dx.doi.org/10.1142/9789812831712\\_0005](http://dx.doi.org/10.1142/9789812831712_0005)
10. Young AT, Betterton EA, Salazar de Rueda L. Photochemical box model for Mexico City. *Atmosfera.* 1997;10:161–178. Available from: <http://www.redalyc.org/pdf/565/56510401.pdf>
11. Kono H, Ito S. A micro-scale dispersion model for motor vehicle exhaust gas in urban areas – OMG Volume-Source model. *Atmos Environ.* 1990;24B:243–251. [http://dx.doi.org/10.1016/0957-1272\(90\)90029-T](http://dx.doi.org/10.1016/0957-1272(90)90029-T)
12. Yamartino RJ, Wiegand G. Development and evaluation of simple models for the flow, turbulence and pollutant concentration fields within an urban street canyon. *Atmos Environ.* 1986;20:2137–2156. [http://dx.doi.org/10.1016/0004-6981\(86\)90307-0](http://dx.doi.org/10.1016/0004-6981(86)90307-0)

13. Gifford FA, Hanna SR. Modelling urban air pollution. *Atmos Environ.* 1973;7:131–136. [http://dx.doi.org/10.1016/0004-6981\(73\)90202-3](http://dx.doi.org/10.1016/0004-6981(73)90202-3)
14. Robeson SM, Steyn DG. Evaluation and comparison of statistical forecast models for daily maximum ozone concentrations. *Atmos Environ.* 1990;24B:303–312. [http://dx.doi.org/10.1016/0957-1272\(90\)90036-T](http://dx.doi.org/10.1016/0957-1272(90)90036-T)
15. Jöckel P, Sander R, Kerker G, Tost H, Lelieveld J, Jöckel P. Technical note: The modular earth submodel system (MESSy): A new approach towards earth system modeling. *Atmos Chem Phys.* 2005;5:433–444. <http://dx.doi.org/10.5194/acp-5-433-2005>
16. Butler TM. Automated sequence analysis of atmospheric oxidation pathways: SEQUENCE version 1.0. *Geosci Model Dev.* 2009;2:145–152. <http://dx.doi.org/10.5194/gmd-2-145-2009>
17. Bloss C, Wagner V, Jenkin ME, Volkamer R, Bloss WJ, Lee LD, et al. Development of a detailed chemical mechanism (MCMv3.1) for the atmospheric oxidation of aromatic hydrocarbons. *Atmos Chem Phys.* 2005;5:641–664. <http://dx.doi.org/10.5194/acp-5-641-2005>
18. Jenkin ME, Saunders SM, Wagner V, Pilling MJ. Protocol for the development of the master chemical mechanism, MCM v3 (Part B): Tropospheric degradation of aromatic volatile organic compounds. *Atmos Chem Phys.* 2003;3:181–193. <http://dx.doi.org/10.5194/acp-3-181-2003>
19. Butler TM, Taraborrelli D, Brühl C, Fischer H, Harder H, Martinez M, et al. Improved simulation of isoprene oxidation chemistry with the ECHAM5/MESSy chemistry-climate model: Lessons from the GABRIEL airborne field campaign. 2008;8:4529–4546. <http://dx.doi.org/10.5194/acp-8-4529-2008>
20. Regelin E, Harder H, Martinez M, Kubistin D, Tatum Ernest C, Bozem H, et al. HOx measurements in the summertime upper troposphere over Europe: A comparison of observations to a box model and a 3-D model. *Atmos Chem Phys.* 2013;13:10703–10720. <http://dx.doi.org/10.5194/acp-13-10703-2013>
21. Stickler A, Fischer H, Bozem H, Gurk C, Schiller C, Martinez-Harder M, et al. Chemistry, transport and dry deposition of trace gases in the boundary layer over the tropical Atlantic Ocean and the Guyanas during the GABRIEL field campaign. *Atmos Chem Phys.* 2007;7:3933–3956. <http://dx.doi.org/10.5194/acp-7-3933-2007>
22. Scorgie Y, Annegarn H, Burger L. Socio-economic impact of air pollution reduction measures – Task 1: Definition of air pollutants associated with combustion processes report. Johannesburg: National Economic Development and Labour Council; 2004.
23. Escience Associates Consulted (Pty) Ltd. The Medium term review of the 2009 Vaal Triangle airshed priority area air quality management plan. Draft review report. Pretoria: Department of Environmental Affairs; 2013.
24. Liebenberg-Enslin H, Hurt Q. Gauteng Province Air Quality Management Plan – Final report. Report No. APP/05/CTMM-02a Rev 3. Johannesburg: Gauteng Department of Agriculture and Rural Development; 2009. Available from: <http://www.gdard.gpg.gov.za/Services1/Air%20Quality%20Management%20Plan.pdf>
25. Jaars K, Beukes JP, Van Zyl PG, Venter AD, Josipovic M, Pienaar JJ, et al. Ambient aromatic hydrocarbon measurements at Welgedund, South Africa. *Atmos Chem Phys.* 2014;14:7075–7089. <http://dx.doi.org/10.5194/acp-14-7075-2014>
26. Derwent R, Jenkin M, Saunders S. Photochemical ozone creation potentials for a large number of reactive hydrocarbons under European conditions. *Atmos Environ.* 1996;30:181–199. [http://dx.doi.org/10.1016/1352-2310\(95\)00303-G](http://dx.doi.org/10.1016/1352-2310(95)00303-G)
27. Jorquera H. Air quality at Santiago, Chile: A box modeling approach I. Carbon monoxide, nitrogen oxides and sulfur dioxide. *Atmos Environ.* 2002;36:315–330. [http://dx.doi.org/10.1016/S1352-2310\(01\)00417-4](http://dx.doi.org/10.1016/S1352-2310(01)00417-4)
28. Liebenberg-Enslin H. A review of existing information on air quality issues related to vehicle emissions in South Africa. Report No.: APP/08/SAPIA Rev 2. Johannesburg: South African Petroleum Industry Association; 2008.
29. Goyns P. Modelling real world driving, fuel consumption and emissions of passenger vehicles: A case study in Johannesburg. Johannesburg: University of Johannesburg; 2008.
30. Menut L, Goussebaile A, Bessagnet B, Khvorostyanov D, Ung A. Impact of realistic hourly emissions profiles on air pollutants concentrations modelled with CHIMERE. *Atmos Environ.* 2012;49:233–244. <http://dx.doi.org/10.1016/j.atmosenv.2011.11.057>
31. European Environment Agency (EEA). EMEP/EEA air pollutant emission inventory guidebook. Copenhagen: EEA; 2009.
32. Blasting TJ. Recent greenhouse gas concentrations. Washington, DC: US Department of Energy, Office of Science; 2013.
33. Gonzalez Abad G, Allen NDC, Bernath PF, Boone CD, Mcleod SD, Manney GL, et al. Ethane, ethyne and carbon monoxide concentrations in the upper troposphere and lower stratosphere from ACE and GEOS-ChemPa comparison study. *Atmos Chem Phys.* 2001;1:9927–9941. Available from: [www.atmos-chem-phys.net/11/9927/2011/](http://www.atmos-chem-phys.net/11/9927/2011/)
34. Diab RD, Raghunandan A, Thompson AM, Thouret V. Classification of tropospheric ozone profile over Johannesburg based on mozaic aircraft data. *Atmos Chem Phys.* 2003;3:713–723. <http://dx.doi.org/10.5194/acp-3-713-2003>
35. Rudolph J. The tropospheric distribution and budget of ethane. *J Geophys Res.* 1995;100:11369–11381. <http://dx.doi.org/10.1029/95JD00693>
36. Logan JA, Prather MJ, Wofsy SC, Mcelroy MB. Tropospheric chemistry: A global perspective. *J Geophys Res.* 1981;86:7210–7254. <http://dx.doi.org/10.1029/JC086iC08p07210>
37. Salby ML. Fundamentals of atmospheric physics. Cambridge: Cambridge University Press; 1996. [http://dx.doi.org/10.1016/S0074-6142\(96\)80037-4](http://dx.doi.org/10.1016/S0074-6142(96)80037-4)
38. Thompson AM, Diab RD, Bodeker GE, Zuncel M, Coetzee GJR, Arher CB, et al. Ozone over southern Africa during SAFARI-92/TRACE A. *J Geophys Res.* 1996;D19(101):23793–23807. <http://dx.doi.org/10.1029/95JD02459>
39. Thompson AM, Balashov NV, Witte JC, Coetzee JGR, Thouret V, Posny F. Tropospheric ozone increases over the southern Africa region: Bellwether for rapid growth in Southern Hemisphere pollution? *Atmos Chem Phys.* 2014;14:9855–9869. <http://dx.doi.org/10.5194/acp-14-9855-2014>
40. Korhenon K, Giannakaki E, Mielonen T, Pfüller A, Laakso L, Vakkari V, et al. Atmospheric boundary layer top height in South Africa: Measurements with lidar and radiosonde compared to three atmospheric models. *Atmos Chem Phys.* 2014;14:4263–4278. Available from: [www.atmos-chem-phys.net/14/4263/2014](http://www.atmos-chem-phys.net/14/4263/2014)
41. Collett KS, Piketh SJ, Ross KE. An assessment of the atmospheric nitrogen budget on the Highveld. *S Afr J Sci.* 2010;106(5/6), Art. #220, 9 pages. <http://dx.doi.org/10.4102/sajs.v106i5/6.220>
42. Hewitt CN. The atmospheric chemistry of sulphur and nitrogen in power station plumes. *Atmos Environ.* 2001;35:387–393. [http://dx.doi.org/10.1016/S1352-2310\(00\)00463-5](http://dx.doi.org/10.1016/S1352-2310(00)00463-5)
43. Venter AD, Vakkari V, Beukes JP, Van Zyl PG, Laakso H, Mabaso D. An air quality assessment in the industrialized western Bushveld Igneous Complex, South Africa. *S Afr J Sci.* 2012;108(9/10), Art. #1059, 10 pages. <http://dx.doi.org/10.4102/sajs.v108i9/10.1059>
44. Sillman S. The relation between ozone, NOx and hydrocarbons in urban and polluted rural environments. *Atmos Environ.* 1999;33:1821–1845. [http://dx.doi.org/10.1016/S1352-2310\(98\)00345-8](http://dx.doi.org/10.1016/S1352-2310(98)00345-8)
45. Stockwell WP, Lawson CV, Saunders E, Goliff WS. A Review of tropospheric atmospheric chemistry and gas-phase chemical mechanisms for air quality modelling. *Atmosphere.* 2012;3:1–32. Available from: <http://www.mdpi.com/2073-4433/3/1/1>
46. Seinfeld J, Pandis S. Atmospheric chemistry and physics: From air pollution to climate change. 2nd ed. New York: Wiley; 2006.
47. Department of Energy. Petroleum Products Act, 1977: Discussion document on the review of fuel specifications and standards for South Africa. Pretoria: Department of Energy; 2011.
48. Amann M, Anderson R, Ashmore M, Depledge M, Derwent D, Grennfelt P, et al. Ground-level ozone in the 21st century: Future trends, impacts and policy implications. London: The Royal Society, 2008. Available from: [http://www.accent-network.org/accent\\_documents/ozone%20report%20web%20pdf%20final.pdf](http://www.accent-network.org/accent_documents/ozone%20report%20web%20pdf%20final.pdf)

